DNA- and Chromatin-Condensing Properties of Rat Testes H1a and H1t Compared to Those of Rat Liver H1bdec: H1t Is a Poor Condenser of Chromatin†

Jyoti R. Khadake‡ and Manchanahalli R. Satyanarayana Rao*,‡,§

Department of Biochemistry, Indian Institute of Science, Bangalore 560 012, India, and Jawaharlal Nehru Centre for Advanced Scientific Research, Indian Institute of Science, Bangalore 560 012, India

Received June 5, 1995; Revised Manuscript Received September 16, 1995⊗

ABSTRACT: Histones H1a and H1t are two major linker histone variants present at the pachytene interval of mammalian spermatogenesis. The DNA- and chromatin-condensing properties of these two variants isolated from rat testes were studied and compared with those from rat liver. For this purpose, the histone H1 subtypes were purified from the respective tissues using both acid and salt extraction procedures. Circular dichroism studies revealed that acid exposure during isolation affects the α-helical structure of both the globular domain (in the presence of 1 M NaCl) and the C-terminal λ-tail (in the presence of 60% trifluoroethanol). The condensation of rat oligonucleosomal DNA, as measured by circular dichroism spectroscopy, by the salt-extracted histone H1 was at least 10 times more efficient than condensation by the acid-extracted histone H1. A site size of 16−20 base pairs was calculated for the salt-extracted histone H1. Among the different histone H1 subtypes, somatic histone H1bdec had the highest DNA-condensing property, followed by histone H1a and histone H1t. All the salt-extracted histones condensed rat oligonucleosomal DNA more efficiently than linear pBR-322 DNA. Histones H1bdec and H1a condensed histone H1-depleted chromatin, prepared from rat liver nuclei, with relatively equal efficiency. On the other hand, there was no condensation of histone H1-depleted chromatin with the testes specific histone H1t. A comparison of the amino acid sequences of histone H1d (rat) and histone H1t (rat) revealed several interesting differences in the occurrence of DNA-binding motifs at the C-terminus. A striking observation is the presence of a direct repeat of an octapeptide motif K(A)T(S)PKKA(S)K(T)K(A) in histone H1d that is absent in histone H1t.

Eukaryotic chromatin is packaged in an interphase nucleus into different levels of ordered structures (Van Holde, 1988). The basic unit of a linear polynucleosome (10 nm filament) can be folded into higher order structure (30 nm filament) which is dependent on both ionic strength and the presence of histone H1. Histone H1 is the most divergent type having several variants. In mammals, seven histone H1 subtypes, namely H1a−e, -°, and -t, have been described (Cole, 1987). Several of these variants are expressed in the same tissue and quite often in the same cell type (Van Holde, 1988; Lennox & Cohen, 1983). It was originally believed that the expression of multiple subtypes of histone H1 in the same cell may not have any functional significance. However, the possibility exists that they modulate locally the higher order structure of chromatin which can then influence DNA transactions at specific loci. This hypothesis is particularly relevant in the context that histone H1 is now being shown to function as a general repressor of gene expression (Weintraub, 1985; Laybourn & Kadanoga, 1991).

During mammalian spermatogenesis, the differentiating germ cells contain different compliments of histone H1 subtypes at various stages of their development (Meistrich et al., 1985). Spermatogonial cells, which are actively undergoing mitosis, contain histone H1a−e. The level of histone H1a, which is a minor component in somatic tissues, is greatly elevated in spermatogonia, constituting approximately 40% of the total histone H1 content. The increase in histone H1a is at the expense of the somatic subtypes H1bde. It is generally observed that histone H1a is associated with actively replicating cells (Lennox & Cohen, 1983). As the germ cells enter the prophase of the meiotic division cycle, a new testis specific variant, histone H1t, is expressed. In mid-pachytene spermatocytes, its level reaches 30% of total histone H1 content (Kremer & Kistler, 1991). The functional significance of the appearance of histone H1t, specifically at the pachytene interval, is not clear. Since the major chromosomal event in pachytene spermatocytes is the meiotic recombination process, it has been suggested that histone H1t may modulate the chromatin structure to facilitate recombination and repair related events. A higher arginine content suggests histone H1t condenses chromatin in a manner analogous to that of histone H5 in chicken erythrocytes (Drabent et al., 1991).

Histone H1 is implicated in the maintenance of chromatin structure at various levels (Widom, 1989). The amino acid sequence of the globular domain of histone H1 is highly conserved among the various histone H1s and is responsible for interacting with the DNA in the chromatosome particle (Thoma et al., 1983; Varga-Weisz et al., 1994). On the other hand, the C-terminal domain, whose sequence diverges considerably among the histone H1 subtypes, has been implicated in the maintenance of the higher order structure of chromatin (Allan et al., 1986). In one of our earlier studies, we had shown that histone H1t is antigenically distinct among the histone H1 subtypes (Markose & Rao, 1985). Histone H1t differs considerably from other histone

† This work was financially supported by the Council of Scientific and Industrial Research, New Delhi.

* Corresponding author: Prof. M. R. S. Rao, Department of Biochemistry, Indian Institute of Science, Bangalore 560 012, India. Fax: 91-080-3341683. Phone: 91-080-3092547.

‡ Department of Biochemistry.

§ Jawaharlal Nehru Centre for Advanced Scientific Research.

⊗ Abstract published in *Advance ACS Abstracts,* November 15, 1995.

0006-2960/95/0434-15792$09.00/0

H1 variants in the amino acid sequences of C-terminal as well as N-terminal tails. These observations suggested that histone H1t may differ in its interaction with chromatin and therefore prompted us to initiate studies on the influence of histone H1t on the structure of chromatin.

One of the consequences of histone H1 binding to DNA, *in vitro*, is the formation of "thick bundles" of nucleoprotein complexes giving rise to what is known as liquid crystals which generate characteristic ψ type circular dichroism spectrum (Fasman et al., 1970; Jordan et al., 1972). The physiological significance of the formation of these thick bundles of histone H1 and DNA complexes is, however, not clear. Using this technique, Liao and Cole (1981) had earlier shown that the individual histone H1 subtypes of calf thymus have different DNA-condensing properties. Moran et al. (1985) have shown that the DNA-condensing property of histone H1 resides in its C-terminal tail. We have, therefore, used the circular dichroism spectroscopic technique in the present study to compare the DNA- and chromatin-condensing properties of histone H1 subtypes (bdec) from rat liver and histones H1a and H1t from rat testes.

Most of the studies on the DNA-condensing properties of histone H1 reported in the literature have been done using acid-extracted histones. We have compared the DNA-condensing properties of histone H1s isolated by acid and salt extraction procedures. The results show that there is a significant difference between histone H1 proteins isolated by these two techniques. Among the various histone H1 subtypes, the testis specific variant, histone H1t, has the least DNA-condensing property. Histone H1t also caused very little condensation of histone H1-depleted chromatin in comparison with other histone H1 subtypes.

MATERIALS AND METHODS

Male albino rats of Wistar strain were used to isolate the various histone H1 subtypes. All the biochemicals were purchased from Sigma Chemical Co. unless otherwise mentioned.

Isolation of Nuclei and Purification of Various Histone H1 Subtypes

Nuclei from rat liver and testes were isolated according to the method of Rao et al. (1982). Histone H1 subtypes were isolated from these nuclei by two different methods described below.

Method I. Total acid soluble proteins of nuclei were extracted with 0.25 N HCl. Histone H1s were extracted from nuclei by the perchloric acid (PCA) extraction method of Johns and Butler (1962). Briefly, nuclei were extracted in 10 volumes of ice-cold 0.75 N PCA by gentle homogenization twice over a period of 30 min. The extracted proteins were precipitated from the supernatant with 25% trichloroacetic acid (TCA). The precipitate was pelleted at 12000× g for 10 min and washed with acidified acetone (containing 0.05% HCl) and acetone. Histones H1bdec represent the somatic variants. For purification of these subtypes, the PCA extract of liver nuclei (10 mg of protein) was dissolved in 0.5 mL of buffer A [50 mM NaCl/20 mM HCl/0.1 mM phenylmethanesulfonyl fluoride (PMSF)/0.002% sodium azide] and chromatographed on a Biogel P-60 (Biorad) column (100 cm × 1.5 cm) equilibrated with buffer A. The column was developed with the same buffer at 4 °C at a flow rate of 6 mL/hr. Fractions (1 mL) were collected, and

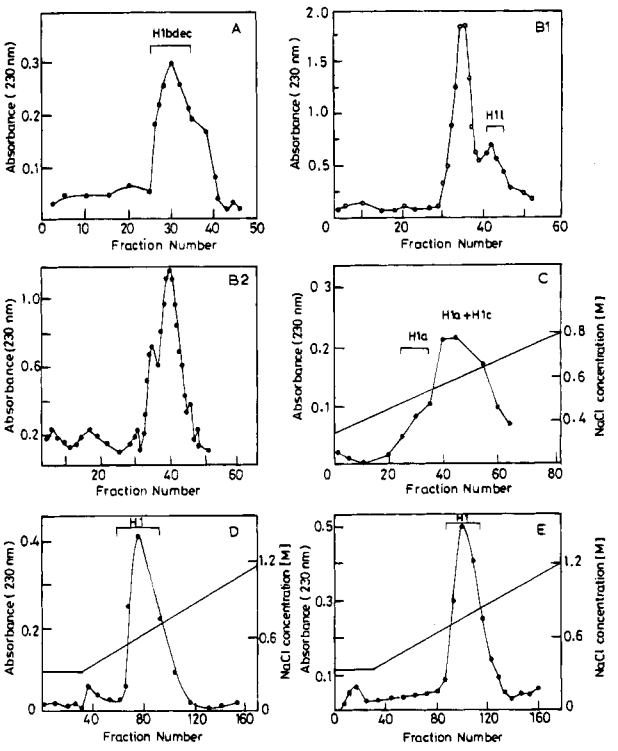

FIGURE 1: Purification of individual histone H1 subtypes from rat liver and testes. (A) Fractionation on Biogel P-60. Liver nuclei were extracted with 0.75 N PCA according to the method of Johns and Butler (1962) as described in Materials and Methods. Approximately 10 mg of protein dissolved in buffer A (50 mM NaCl/20 mM HCl/ 0.1 mM PMSF) was chromatographed on a Biogel P-60 column (100 cm × 1.5 cm) equilibrated with buffer A. Fractions (1 mL) were collected, and absorbance was monitored at 230 nm. The peak fractions marked by the bracket were pooled and processed further as described in Materials and Methods. (B1) Fractionation of PCA-extracted histone H1s from testicular nuclei on Biogel P-60. Approximately 7 mg of protein was processed as described in the legend to part A. The fractions under the small hump marked by the bracket containing predominantly histone H1t from two such columns were pooled and rechromatographed on the Biogel P-60 column. The pattern shown in part B2 shows the profile of this second column. The major peak between fractions 38 and 44 which contained only histone H1t were pooled and concentrated. (C) The fractions under the major peak of Figure 1B1 (fractions 32−37) which conained histones H1a and H1c were pooled and chromatographed on CM Sephadex G-25 as mentioned in Materials and Methods. The proteins were dissolved in buffer B (25 mMTris-HCl (pH 8.8)/ 0.1 mM PMSF) containing 0.35 M NaCl and applied on a preequilibrated column of CM Sephadex G-25. The column was developed with a linear 100 mL gradient of 0.35 to 0.80 M NaCl in buffer B. Fractions (1 mL) were collected and monitored for absorbance at 230 nm. Fractions between 26 and 35 contained pure histone H1a. (D) Fractionation of testicular histone H1 on CM Sephadex G-25. Soluble chromatin was prepared from testicular nuclei and processed on CM Sephadex G-25 as in Figure 1D and method II. Fractions between 65 and 95 were pooled, dialyzed against 1% acetic acid, and lyophilized. The protein sample was then fractionated on Biogel P-60, and the pattern was similar to that obtained in Figure 1B2. The major peak of the Biogel P-60 column was processed on a second CM Sephadex G-25 column as described in the legend to part C to obtain histone H1a. (E) Fractionation of liver histone H1 on CM Sephadex G-25. Liver nuclei were digested with micrococcal nuclease to generate soluble chromatin. Histone H1s in this soluble chromatin were bound to CM Sephadex G-25 according to the method of Garcia-Ramirez et al. (1990) and further fractionated on a linear gradient of 0.35 to 1.2 M NaCl as mentioned in method II. Fractions (1 mL) were collected and monitored for absorbance at 230 nm. The peak fractions (90−115) were pooled and rechromatographed on a Biogel P-60 column as described in the legend to part A.

the absorbance was monitored at 230 nm (Figure 1A). The peak fractions were pooled, precipitated with 20% TCA, washed with acidified acetone and acetone, and stored dry. For purification of histone H1t, the PCA extract of testicular nuclei (7 mg) was chromatographed on a Biogel P-60 as described above for H1bdec (Figure 1B). Two absorbance peaks were obtained. The first peak contained mainly histones H1a and H1c, while the second smaller peak contained predominantly histone H1t (Markose & Rao, 1985). The proteins of the second peak were rechromatographed on the Biogel P-60 column. The peak fractions were pooled, precipitated with 20% TCA, washed with acidified acetone and acetone, and stored dry. Histone H1a present in the major peak of the first column was further purified on a column of CM Sephadex G-25 according to the method of Garcia-Ramirez et al. (1990) with minor modifications. Briefly, the sample was dissolved in 0.35 M NaCl in buffer B (25 mM Tris-HCl (pH 8.8)/0.1 mM PMSF) and applied to a 10 mL packed column volume of CM Sephadex G-25 (Pharmacia) equilibrated in loading buffer and then developed with a 100 mL gradient of 0.35 to 0.80 M NaCl in buffer B (Figure 1C). Fractions (1 mL) were collected, and absorbance at 230 nm was recorded. Every third fraction of the hump observed in the column profile was analyzed on a sodium dodecyl sulfate (SDS)−10% polyacrylamide gel (Laemmli, 1970). The fractions showing a single band of histone H1a were pooled, precipitated with 20% TCA, washed with acidified acetone and acetone, and stored dry.

Method II. In one of our earlier studies (Markose & Rao, 1985), we had purified histone H1t from rat testes after extraction of H1s from testicular nuclei with 0.6 M NaCl. However, when we tried to purify larger amounts of individual histone H1 subtypes, we encountered degradation of histone H1s. Therefore, we adapted the method of Garcia-Ramirez et al. (1990) for the purification of histone H1 subtypes. Briefly, nuclei isolated from the testes of 40-day-old rats were digested with micrococcal nuclease (Worthington, 40 units/100 A_{260} units of nuclei for 30 s at 37 °C). The digestion was arrested by addition of EGTA to a final concentration of 10 mM. Following centrifugation, the nuclear pellet was resuspended in 10 mM Tris-HCl (pH 8.0)/10 mM EDTA. The chromatin released was collected as supernatant after centrifugation at 10000*g* and diluted to 20 A_{260} units/mL with 0.25 mM EDTA (pH 7). The NaCl concentration was adjusted to 0.35 M by the dropwise addition of 4 M NaCl with constant gentle shaking. CM Sephadex G-25 (12 mg of beads/mL) was added to the chromatin suspension and the mixture kept on ice for 2 h with occasional mixing. At this step, histone H1s are selectively removed from chromatin and bound to CM Sephadex resin. The beads were collected by centrifugation at 10000*g* for 10 min. After the beads were washed twice with 0.35 M NaCl/10 mM Tris-HCl (pH 8.0)/0.1 mM phenylmethanesulfonyl fluoride, the final suspension of the beads was overlaid on a column of CM Sephadex G-25 (45 mL) which had been preequilibrated with 0.35 M NaCl/10 mM Tris-HCl (pH 8.8)/0.1 M PMSF. The bound histone H1s were eluted with a 120 mL linear gradient of 0.35 to 1.2 M NaCl in the same buffer (Figure 1D). Fractions (1 mL) were collected, and absorbance at 230 nm was recorded. The peak fractions were pooled, dialyzed against 1% acetic acid, and lyophilized. The testicular histone H1 thus obtained from the CM Sephadex G-25 column was then fractionated on a Biogel P-60 column as described in method I. The first peak was processed further on a second CM Sephadex G-25 column with a linear gradient of NaCl from 0.35 to 0.8 M to obtain histone H1a, while the second peak was rechromatographed on a second Biogel P-60 column to yield histone H1t.

To obtain histone H1bdec, liver nuclei were digested with micrococcal nuclease and processed as described above for testis histone H1 and chromatographed on CM Sepahdex G-25 using a linear 120 mL gradient of NaCl from 0.35 to 1.2 M (Figure 1E). The peak fractions were pooled, dialyzed against 1% acetic acid, lyophilized, and rechromatographed on a Biogel P-60 column as described in Method I. At no time were these histone H1s exposed to strong acids or organic solvents (the lowest pH was 3.5−4.0 during dialysis against acetic acid and gel permeation chromatography on Biogel P-60). In all cases, the purified protein fractions were pooled, dialyzed against 1% acetic acid, lyophilized, and stored dry at −20 °C. Storage of purified histone H1s without dialysis against acetic acid and lyophylization led to partial degradation of the proteins.

Preparation of DNA Samples

Escherichia coli HB101 cells harboring pBR-322 were used to isolate DNA by the alkali lysis method followed by purificaton by the cesium chloride density gradient centrifugation method (Sambrook et al., 1989). Linear pBR-322 DNA was prepared by digestion of this DNA with restriction endonuclease *Eco*RI (Bangalore Genei, Bangalore). Rat oligonucleosomal DNA was prepared from rat liver nuclei as described by Rao et al. (1982). Briefly, purified nuclei were digested with micrococcal nuclease (Worthington, 40 units/100 A_{260} units of nuclei for 2 min at 37 °C) to 5% acid solublity, and the oligonucleosomes released after treatment with 10 mM EDTA were digested with 10 μg/mL proteinase K (Sigma) and extracted with phenol/chloroform and chloroform. Oligonucleosomal DNA of different sizes was prepared by electroelution followed by extraction with phenol/chloroform and chloroform. All the DNA samples were checked for their purity as judged by electrophoresis on a 1.2% agarose gel, the ultraviolet spectrum, and the A_{260}/A_{280} ratio.

Preparation of Histone H1-Stripped Chromatin

Histone H1-stripped chromatin was prepared from rat liver nuclei according to the method of Allan et al. (1980). Briefly, polynucleosomes were obtained from liver nuclei after micrococcal nuclease digestion as described above. After treatment with pancreatic ribonuclease A (Sigma), the polynucleosomes were fractionated on a linear 5 to 40% sucrose density gradient in a Beckman L7-55 ultracentrifuge with a SW 28 rotor (26 000 rpm, 22 h). The gradients were fractionated in an ISCO 185 density gradient fractionator, and the DNA in individual fractions was analyzed by electrophoresis on an agarose gel. The fractions containing DNA ranging from 2 to 6 kbp (kilobase pairs) (10 to 30 oligomers) were pooled, dialyzed against TEP buffer [10 mM Tris-HCl (pH 7.5)/0.1 mM EDTA/0.2 mM PMSF] containing 10 mM NaCl and stored at 4 °C. Histone H1 and nonhistone proteins were removed from this native chromatin by passage over a double-stranded (ds) DNA−cellulose column (12 mg of DNA/g of CF 11 cellulose; Weissbach &

Poonian, 1974). Chromatin (0.5 mg) was suspended in TEP buffer containing 80 mM NaCl at a concentration of 1.5 A_{260}/mL and mixed with 5 mL of ds DNA−cellulose pellet (1 g of cellulose). The binding was facilitated by end to end shaking for 17−20 h at 4 °C.

Histone H1-stripped chromatin was collected from the supernatant after centrifugation at 5000*g* for 10 min. H1-stripped chromatin was stored in aliquots at −20 °C. The authenticity of the H1-stripped chromatin was checked by (a) analysis of acid soluble proteins and (b) micrococcal nuclease digestion pattern. The histone/DNA ratio of native chromatin was 0.83 (w/w), while that of H1-stripped chromatin was 0.70 (w/w).

Circular Dichroism Studies

The circular dichroism (CD) spectrum of individual purified histone H1 subtypes was recorded at a protein concentration of 200 μg/mL in either (a) 10 mM sodium phosphate (pH 7.5), or (b) 1 M NaCl in 10 mM sodium phosphate (pH 7.5), or (c) 10 mM sodium phosphate (pH 7.5) containing 60% 2,2,2-trifluoroethanol (TFE). The spectra were recorded at room temperature on a Jasco model J 500 A spectropolarimeter attached to a computer using a 1 mm path length quartz cuvette and a slit width of 0.5 mm. Mean amino acid residue weight of 98.9 was used for calculation of the molar ellipticity values of proteins. The α-helical content in different histone H1 subtypes was estimated from θ values at 220 nm using the formula, $\theta = 3300\Delta E$ and percent helicity = $\Delta E - 0.25/0.105$ as described by Clark et al. (1988). Complexes of various DNA samples and the different histone H1 subtypes were prepared by direct mixing in 150 mM NaCl/10 mM Tris-HCl (pH 7.4)/0.1 mM EDTA. Increasing aliquots of a solution containing the individual histone H1 subtypes were added to DNA. After the complexes were incubated at room temperature for 10 min, the spectra were recorded in a Jasco J20 spectropolarimeter using a cuvette of 1 cm path length.

There was no change in the spectrum after 10 min, indicating that it represents the complex formed at equilibrium. A mean nucleotide residue weight of 330 was used for calculation of the molar ellipticity values of DNA. The absorbances of the nucleoprotein complexes were routinely checked at 320 nm and were in the range of 0.002−0.004, indicating that they did not form insoluble aggregates.

To study the effect of salt concentration on the condensation of DNA brought about by the individual salt-extracted histone H1 subtypes, protein−DNA complexes were made in 5 mM Tris-HCl (pH 7.5) and 1 mM EDTA containing NaCl varying from 0 to 0.5 M and left overnight at 4 °C, after which the spectra were recorded as described above. In order to study the effect of individual histone H1 subtypes on condensation of histone H1-stripped chromatin, the depeleted chromatin was mixed with increasing concentrations of histone H1 subtype in 80 mM NaCl, 10 mM Tris-HCl (pH 7.5), and 0.1 mM EDTA. The spectra were recorded after the sample was kept overnight at 4 °C.

Analytical and Other Methods

Protein concentrations were determined by the turbidometric method (Platz et al., 1977). Histone H1 concentrations were also estimated using the formula $A_{230nm} = 1.85$ for 1 mg/mL protein (Camerini-Otero et al., 1976). Electrophoretic analysis of histones was made on a SDS−polyacrylamide gel (Laemmli, 1970). Secondary structure predictions were generated using the CF and GOR algorithms.

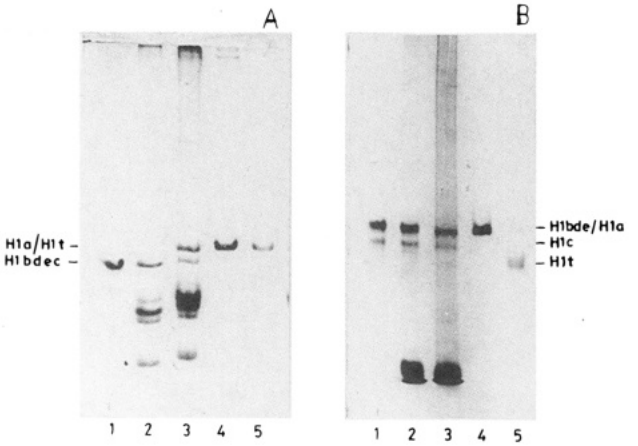

FIGURE 2: Polyacrylamide gel electrophoretic pattern of purified histone H1 subtypes. Panel A shows a 10% acid−urea polyacrylamide gel stained with Naphthol Blue Black, and panel B shows a 10% sodium dodecyl sulfate−polyacrylamide gel stained with Coomassie Brilliant Blue R: lane 1, histone H1-bdec; lane 2, 0.25 N HCl extract of liver nuclei; lane 3, 0.25 N HCl extract of rat testicular nuclei; lane 4, histone H1a; and lane 5, histone H1t. Histones H1a and H1t comigrate in acid−urea gel, whereas they were well-separated in SDS−PAGE.

RESULTS

The main emphasis of the present investigation was comparison of the DNA- and chromatin-condensing properties of histones H1a and H1t present in rat testes. Although there is considerable discussion in the literature that exposure to strong acids like perchloric acid and trichloroacetic acids or even organic solvents like acetone may partially denature the histone H1s, much of the information on DNA- and chromatin-condensing properties has been obtained with acid-extracted histone H1s. Therefore, we decided to make a systematic study to compare the acid-extracted histone H1 subtypes and salt-extracted histone H1 subtypes in their ability to condense DNA. For this purpose, we developed a strategy for the purification of the histone H1 subtypes from rat liver and testes by adapting the recently described method of Garcia-Ramirez et al. (1990). The electrophoretic patterns of the purified histone H1 subtypes are shown in Figure 2. There was no difference in the electrophoretic mobility of the histone H1 subtypes purified by the two methods. The liver histone H1s were comprised of the subtypes H1bdec and were used as such without any attempt to further purify each of these subtypes (see below).

Circular Dichroism Sepctra of Histone H1 Subtypes. Histone H1 attains its optimal secondary structure in terms of its α-helical content in the presence of greater than 150 mM NaCl. Since there is no simple functional assay for histone H1, the salt-induced helical content is often taken as an index of the native state of the purified protein. If the acid exposure would have caused an irreversible denaturation during isolation by method I, it would be reflected in the secondary structure properties. We, therefore, analyzed the secondary structure of the purified histone H1 subtypes by determining the α-helical content using the circular dichroism technique. The spectra of the proteins are shown in Figure

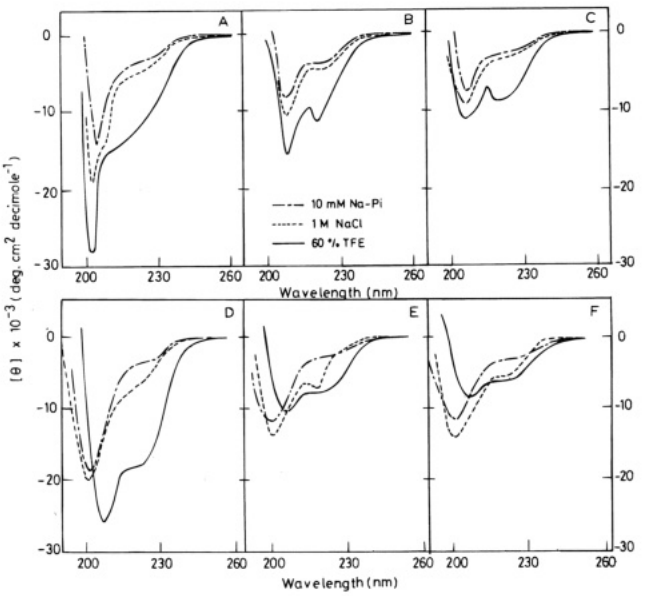

FIGURE 3: Circular dichroism spectra of purified histone H1 subtypes. Panels A−C represent spectra of acid-extracted histone H1 subtypes, while D−F represent the spectra of salt-extracted proteins: A and D (H1bdec), B and E (H1a), and C and F (H1t). A 200 μg/mL solution of purified histone H1 subtypes was used for recording the CD spectrum in a Jasco 500A spectropolarimeter as mentioned in the text. The spectra were recorded in (a) 10 mM $NaPO_4$ (− - −), (b) 10 mM $NaPO_4$ containing 1 M NaCl (- - -), and (c) 10 mM $NaPO_4$ containing 60% TFE (—).

Table 1: Percentage α-Helicity Induced in Different Histone H1 Subtypes[a]

		θ_{220nm}		Σ		% helicity	
protein	solvent	acid[b]	salt[c]	acid	salt	acid	salt
H1bdec	10 mM $NaPO_4$	−3954	−3639	1.19	1.10	8.9	8.10
	1 M NaCl	−4933	−6330	1.48	1.92	11.7	16.01
	60% TFE	−12053	−17660	3.62	5.35	32.1	48.60
H1a	10 mM $NaPO_4$	−4357	−2914	1.30	0.88	10.1	6.00
	1 M NaCl	−4352	−7210	1.36	2.16	10.6	18.20
	60% TFE	−10969	−7788	3.29	2.36	29.0	20.10
H1t	10 mM $NaPO_4$	−3964	−2815	1.19	0.85	9.0	5.70
	1 M NaCl	−3932	−5619	1.18	1.70	9.0	13.80
	60% TFE	−8497	−5655	2.55	1.71	21.9	13.90

[a] The percent α-helicity was calculated according to the method of Clark et al. (1988). The values shown are an average of three independent experiments. [b] Histone H1 isolated by acid extraction (method 1). [c] Histone H1 isolated by the salt method (method 2).

3A−F. For each of the histone H1 subtypes, the spectrum was recorded in (a) 10 mM sodium phosphate (pH 7.5), (b) 1 M NaCl/10 mM sodium phosphate (pH 7.5), and (c) 60% TFE/10 mM sodium phosphate (pH 7.5). All three histone H1 subtypes showed a characteristic α-helical spectrum at 222 nm. It is seen that, even in 10 mM sodium phosphate, a fair amount of α-helicity was induced which was further enhanced in 1 M NaCl. The percentages of α-helicity calculated from θ_{222nm} values are given in Table 1. Several important observations can be made from this table. There is a considerable difference in the α-helicity induced in the presence of 1 M NaCl between the acid-extracted and salt-extracted histone H1 subtypes. For example, the salt-extracted histone H1bdec attained 16.08% helicity in 1 M NaCl as compared to 11.7% for acid-extracted histone H1bdec. Similarly, salt-extracted histones H1a and H1t showed higher helical content than the acid-extracted proteins. The α-helical content induced in 1 M NaCl is

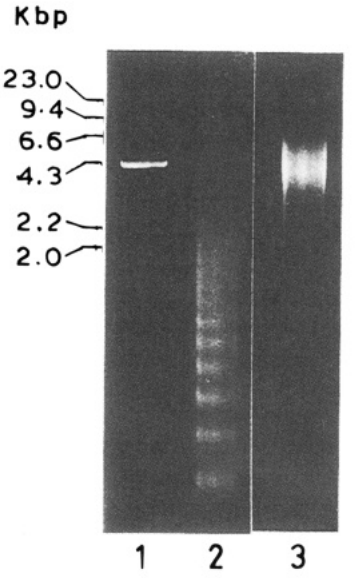

FIGURE 4: Electrophoretic pattern of DNA samples used in the preparation of histone H1−DNA complexes. The DNA samples were run on a 1.2% agarose gel in TAE buffer: lane 1, linear pBR-322 DNA; lane 2, rat liver oligonucleosomal DNA; and lane 3, 2−5 kbp rat oligonucleosomal DNA.

contributerd by the globular domain of the histone H1 molecule. These results suggest that the globular domain of acid-extracted histone H1 may have undergone partial irreversible denaturation during exposure to strong acids and/or organic solvents. The observation that a small but significant helical content was obtained even in the absence of 1 M NaCl has been explained as being contributed by phosphate ions having specific binding sites on histone H1 (De Petrocellis et al., 1986). It is also evident that the α-helicity induced in histone H1t in the presence of 1 M NaCl is much less than that observed with either histone H1bdec or H1a. While the α-helicity observed in the presence of 1 M NaCl reflects the secondary structure attained by the globular domain, the α-helicity observed in the presence of 60% TFE includes additional regions which can be induced to attain the α-helical structure. Clark et al. (1988) have shown that this enhanced α -helical structure in 60% TFE resides in the C-terminal tail of histone H1. It is interesting to note that the additional α-helicity induced in 60% TFE is lower for histones H1a and H1t than for histone H1bdec. It is believed that this induced α-helicity observed in the presence of TFE may be stabilized upon binding to DNA. Again here, the acid-extracted histone H1 subtypes differed considerably from salt-extracted histone H1 subtypes.

Circular Dichroism Spectral Studies on the Interaction of Histone H1 Subtypes with DNA. In one of the very early studies, Liao and Cole (1981) showed that the different histone H1 subtypes from calf thymus isolated by the acid extraction method differ in their DNA condensation properties. The extent of condensation also depended on the type of DNA used. In the present studies, we have used two types of DNA, (a) rat oligonucleosomal DNA (2−5 kbp) representing the DNA from rat and (b) linear pBR-322 representing nonhomologous prokaryotic DNA, to compare the DNA-condensing properties of histones H1bdec, H1a, and H1t. The electrophoretic pattern of DNA used in these studies is shown in Figure 4. Since we observed considerable differences in the secondary structure of histone H1 subtypes

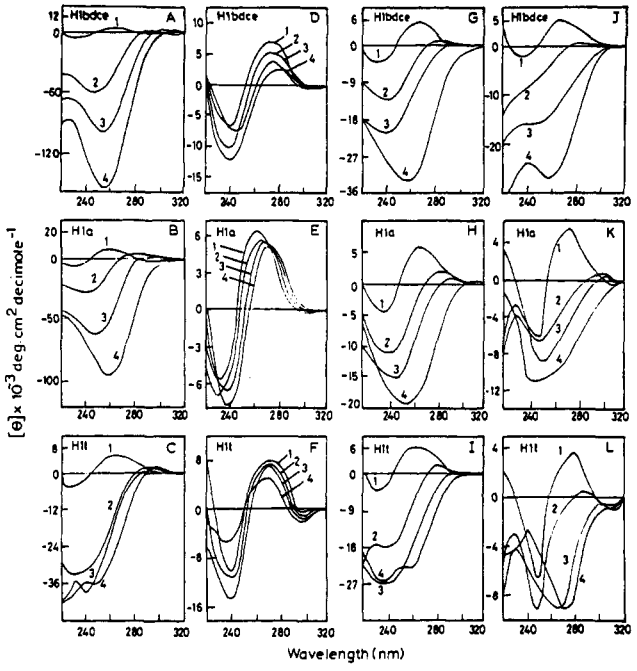

FIGURE 5: Circular dichroism spectra of histone H1−DNA complexes. The spectra of the various protein−DNA complexes prepared at different histone H1/DNA ratios, as mentioned in the text, in 150 mM NaCl/5 mM Tris-HCl (pH 7.5)/0.1 mM EDTA, were recorded in a Jasco model J20 spectropolarimeter: panels A−F, rat oligonucleosomal DNA; panels G−L, linear pBR 322 DNA; panels A−C and G−I, salt-extracted histones H1; and panels D−F and J−L, acid-extracted histone H1s. Curve 1 in all figures represents the DNA spectrum. Curves 2−4 represent the spectra with histone/DNA ratios (mole/bp) of 0.038, 0.05, and 0.058 (panel A); 0.032, 0.04, and 0.056 (panel B); 0.03, 0.038, and 0.045 (panel C); 0.015, 0.032, and 0.045 (panel G); 0.02, 0.038, and 0.05 (panels H and I); and 0.003, 0.005, and 0.006 (panels D−F and J−L).

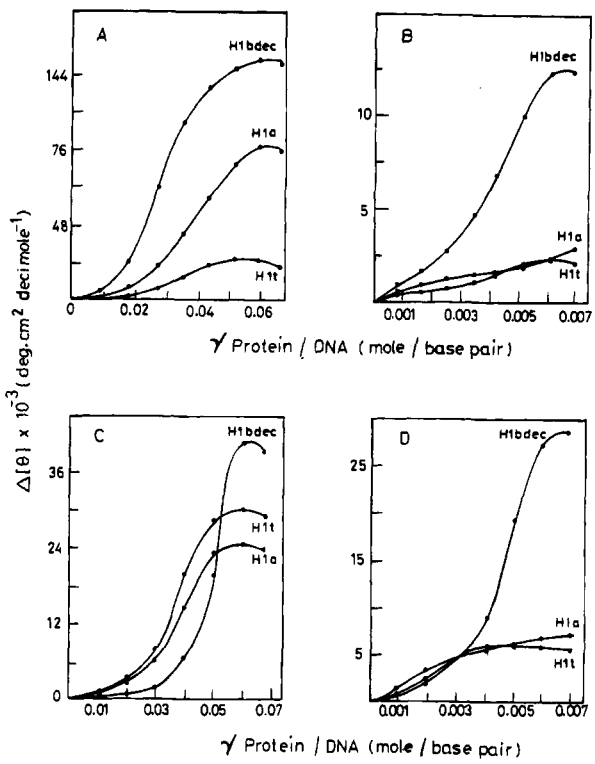

FIGURE 6: Effect of histone H1 subtypes on the condensation. Rat oligonucleosomal DNA (panels A and B) and linear pBR 322 DNA (panels C and D). Ellipticity changes observed in Figure 5 with the two types of nucleic acids upon binding to histone H1 subtypes, termed $\Delta\theta$, are plotted as a function of protein/DNA ratio (mole/bp). Panels A and C represent the data obtained with salt-extracted histone H1 subtypes, while B and D represent the data with acid-extracted histone H1 subtypes.

isolated by the acid and salt extraction methods, we asked whether such differences would also influence DNA-condensing properties. The circular dichroism spectra of the two DNA samples with increasing concentrations of the different histone H1 subtypes are shown in Figure 5A−F (2−5 kbp rat oligonucleosomal DNA) and Figure 5G−L (linear pBR-322 DNA). The spectrum of the two DNA samples is characteristic of the B type DNA. Addition of increasing concentrations of all the histone H1 subtypes progressively decreased the positive θ_{270nm} and generated theψ type spectrum. The molecular basis of the formation of the ψ type of spectrum is, however, not clear.

It is generally believed that histone H1 molecules pack the DNA duplexes into ordered aggregates in the form of liquid crystals. Although all the subtypes generated the ψ type of spectrum, the absolute value of negative θ_{270nm} generated varied with the type of histone H1 subtypes used and also with the type of DNA. Furthermore, it is clearly evident that salt-extracted histone H1s were much more effective in generating the ψ type of spectrum than the acid-extracted histone H1s. There was no significant change in the absorbance at 320 nm even at the highest concentration of histone H1, indicating that the nucleoprotein complexes did not form insoluble aggregates. For a better understanding of the effect of the individual histone subtypes on DNA condensation, the decrease in θ_{270nm} upon each addition of the individual histone H1 subtypes to free DNA, termed $\Delta\theta_{270nm}$, was plotted against r value (protein/DNA ratio, mole/bp), and these results are presented in Figure 6A−D.

From a comparison of the curves presented in Figure 6A,B, it is clear that the net condensation observed at saturation with H1bdec is much higher than that with either histones H1a or H1t. Similar observations were made with both salt-extracted and acid-extracted histone H1 subtypes. However, there are two important differences in the DNA-condensing properties between salt-extracted and acid-extracted histone H1 subtypes. Firstly, the absolute $\Delta\theta$ observed at saturation (refer to the y axis) is nearly 10-fold higher with salt-extracted histone H1 subtypes than with the acid-extracted proteins. Secondly, the condensation with acid-extracted histone H1 subtypes is initiated at a much lower r value (mole of protein/bp), namely 0.001, and reaches a saturation at an r value of 0.006. However, with salt-extracted histone H1bdec, the condensation begins only with an r value of 0.01 and reaches a saturation at 0.06. This would imply that many more histone H1 molecules are loaded on DNA duplexes before packing is initiated in the case of salt-extracted histone H1. In fact, Clark and Thomas (1986) have shown that the binding of histone H1 to DNA is highly cooperative in nature. From the r values at saturation, it can also be calculated that one molecule of H1bdec (salt-extracted) occupies approximately 16−20 bp of DNA which is drastically affected in the case of acid-extracted histone H1 (apparent site size of 160−200 bp). The relative efficiencies of condensation of linear pBR-322 DNA with different histone H1 subtypes are shown in Figure 6C,D. The basic condensation properties observed are very similar to that of homologous oligonucleosomal DNA in that (a) salt-extracted histone H1s have better DNA-condensing proper-

ties than acid-extracted proteins and (b) histone H1bdec is more efficient than the variant histones H1a and H1t.

However, a more important observation is that the net condensation θ observed at saturation with respect to linear pBR-322 DNA ($-40\,000°\cdot cm^2\cdot dmol^{-1}$) is very much lower than that observed with homologous oligonucleosomal DNA ($-150\,000°\cdot cm^2\cdot dmol^{-1}$). These results suggest that the condensation of eukaryotic DNA by histone H1 is more efficient than prokaryotic DNA, probably implying some sequence preference shown by histone H1 in its DNA-condensing property. Since we have used oligonucleosomal DNA of 2−5 kbp (which is approximately equivalent to the length of pBR-322 DNA), we do not believe that the differences observed in the condensation of two DNA samples are because of different chain lengths of the two DNA samples. We would like to point out here that histone H1 has been reported to interact with eukaryotic DNA more selectively than prokaryotic DNA (Renz et al., 1975). Furthermore it is now fairly established that histone H1 interacts specifically with AT rich DNA sequences, particularly those associated with nuclear scaffold (Kas et al., 1989). Recently, histone H1e was shown to bind preferentially a GC rich sequence (Wellman et al., 1994).

Effect of Ionic Strength on DNA Condensation by Histone H1 Subtypes. All the above circular dichroism spectral studies were carried out in a buffer containing 150 mM NaCl. Since histone−DNA interactions are significantly influenced by the ionic strength of the buffer, it was necessary to study the effect of NaCl concentration on DNA condensation brought about by histones H1bdec, H1a, and H1t to rule out the possibility that these subtypes might have different optimum NaCl concentrations that bring about maximum condensation. For this purpose, we recorded the circular dichroism spectra of histone H1−DNA complexes (rat oligonucleosomal DNA) at an r value of 0.04 (mole/bp) in the presence of increasing concentrations of NaCl.

The experiments described above have clearly shown that salt-extracted histone H1s are better than acid-extracted histone H1s, and hence, all the subsequent experiments were carried out with salt-extracted histone H1 subtypes. The results of these studies are shown in Figure 7. In the case of histone H1bdec, the maximum $\Delta\theta$ was observed between 0.15 and 0.20 M NaCl. A decrease in the condensation observed beyond 0.3 M NaCl is seen because the histone−DNA complexes start dissociating at higher ionic strength. It is also evident from the figure that the optimum salt concentration for condensation of DNA by histones H1a and H1t also lies between 0.15 and 0.2 M NaCl. There was no change in the absorbance at 320 nm of histone H1 and DNA complexes at different NaCl concentrations. Thus, the low DNA-condensing properties of the rat histones H1a and H1t observed in the present study are not because of an altered ionic strength requirement of these proteins for maximum condensation of DNA. It may be pertinent to mention here that, at 0.4 M NaCl concentration, the B type spectrum of DNA was regenerated, indicating that there is no gross alteration in the secondary structure of DNA during the condensation process.

Effect of Histone H1 Subtypes on Condensation of H1-Depleted Chromatin. All the experiments described above dealt with the DNA condensation properties of the histone H1 subtypes with naked duplex DNA. Since, *in vivo*, the target of interaction for histone H1 is nucleosomes, we next

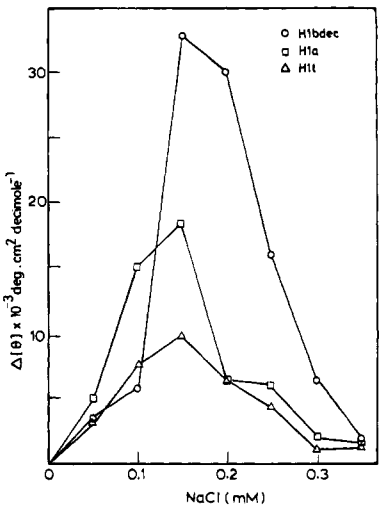

FIGURE 7: Effect of ionic strength on the condensation of DNA by histone H1 subtypes. Rat oligonucleosomal DNA (2−5 kbp) was incubated with different histone H1 subtypes (salt-extracted) at a protein/DNA ratio of 0.04 (mole/bp) overnight in 10 mM Tris-HCl (pH 7.5) and 0.1 mM EDTA containing 0−0.5 M NaCl. The ellipticity changes $\Delta\theta$ at 270 nm were plotted against NaCl concentration.

investigated the chromatin-condensing properties of the individual histone H1 subtypes. For this purpose, we prepared the histone H1-depleted chromatin from rat liver. The basic structural and biochemical properties of the histone H1-depleted chromatin are shown in Figure 8. SDS−polyacrylamide electrophoresis of the acid soluble proteins clearly revealed the absence of histone H1s in this preparation (Figure 8B). Micrococcal nuclease digestion of histone H1-depleted chromatin also revealed the integrity of the polynucleosome structure (Figure 8C). As expected, the positive ellipticity at 270 nm of histone H1-depleted chromatin increased to $2000°\cdot cm^2\cdot dmol^{-1}$ from that of $800°\cdot cm^2\cdot dmol^{-1}$ for native chromatin. The CD spectra of the histone H1-depleted chromatin after addition of salt-extracted histones H1bdec, H1a, and H1t are shown in Figure 8D. Addition of histone H1bdec (Figure 8D) at a ratio of 0.0032 (mole/bp; approximately 1 molecule/2 nucleosomes) resulted in a substantial decrease in θ_{270nm} ($960°\cdot cm^2\cdot dmol^{-1}$). At an input ratio of 0.0064, equivalent to 1 molecule of histone H1/nucleosome, the positive ellipticity at 270 nm was similar to that of the native chromatin ($720°\cdot cm^2\cdot dmol^{-1}$). Addition of histone H1a to histone H1-depleted chromatin at similar ratios resulted in a decrease in the positive ellipticity at 270 nm to give θ_{270nm} of $995°\cdot cm^2\cdot dmol^{-1}$ at a ratio of 0.0032 mole/bp and $850°\cdot cm^2\cdot dmol^{-1}$ at a ratio of 0.0064 mole/bp (Figure 8D). However, the most striking observation was made with histone H1t (Figure 8D). Addition of histone H1t to histone H1-depleted chromatin did not result in any decrease in the positive ellipticity at both input ratios of 0.0032 and 0.0064 (mole/bp). In all these experiments, there was no significant change in the absorbance at 320 nm, indicating that the histone H1−chromatin complexes being studied were not in the form of insoluble aggregates.

DISCUSSION

The results presented in this paper concern the DNA- and chromatin-condensing properties of two major linker histones present in the testes, namely histone H1a and H1t. Histone H1a is predominantly expressed in spermatogonial cells

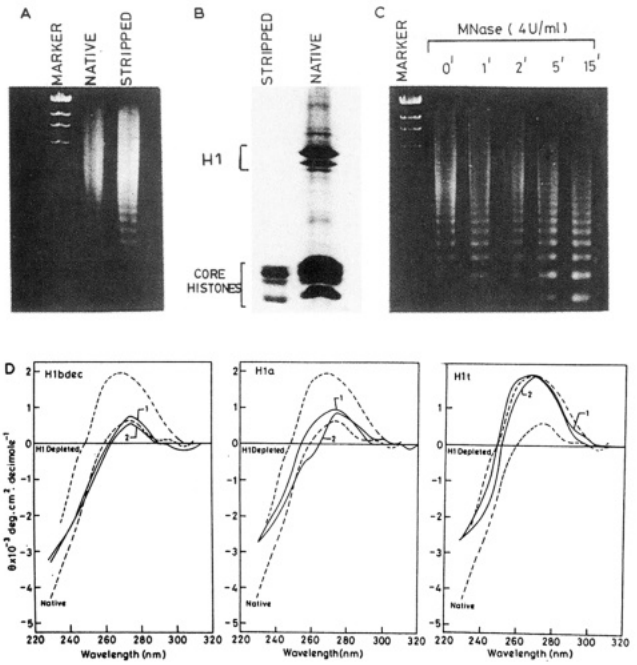

FIGURE 8: Effect of salt-extracted histone H1 subtypes on the circular dichroism spectra of histone H1-depleted chromatin. Polynucleosomes (10−30 mers) were prepared from soluble chromatin of rat liver by centrifugation on a linear 5 to 40% sucrose density gradient as described in the text. Histone H1 was stripped off the chromatin using ds DNA cellulose according to the method of Allan et al. (1990). (A) Electrophoretic pattern of DNA before and after stripping of histone H1. Marker lane represents λ-DNA digested with *Hin*dIII. (B) SDS−PAGE of proteins associated with native and stripped chromatin. (C) Micrococcal nuclease digestion pattern of H1-depleted chromatin. (D) Circular dichroism spectra of histone H1-depleted chromatin after complexing with different histone H1 subtypes. Histone H1-depleted chromatin was mixed with two concentrations of individual histone H1 subtypes (salt-extracted) in 80 mM NaCl/10 mM Tris-HCl (pH 7.5)/0.1 mM EDTA. The spectra were recorded after the sample was kept overnight at 4 °C: 1, histone/DNA ratio of 0.0032 (mole/bp); and 2, histone/DNA ratio of 0.0064 (mole/bp).

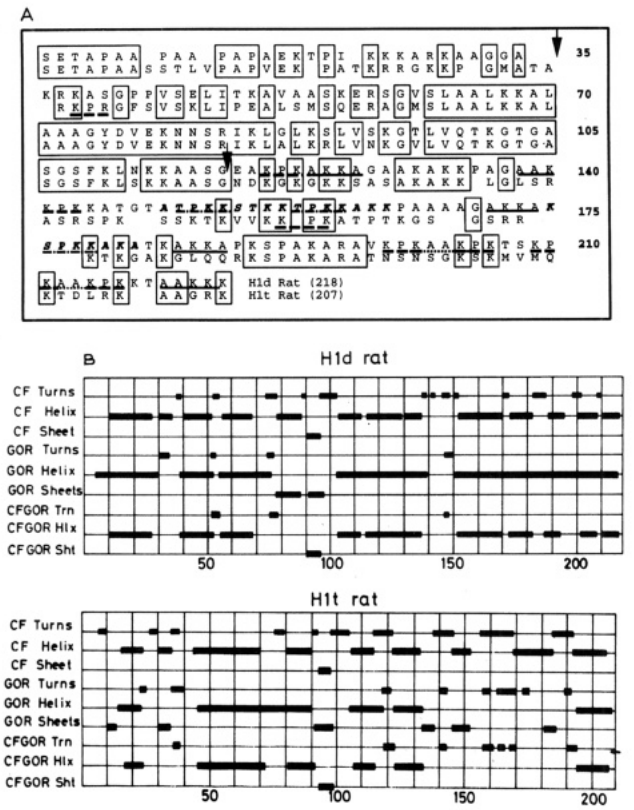

FIGURE 9: (A) Comparison of the amino acid sequences of rat histones H1d and H1t. The original sequence of H1d reported by Cole et al. (1990) has recently been corrected by Drabent et al. (1993) who have found two additional alanine residues at position 160. The rest of the sequence reported by these two groups of workers is identical. Alignment of the sequence of amino acids of histone subtypes is based on the homology stretches. The boxed regions indicate the identity. The globular domain of the histone H1 is the region between the two arrows. The sequences before the first arrow and after the second arrow indicate the N-terminus and the C-terminus of the protein, respectively. Various DNA binding motifs discussed by Churchill and Travers (1991), namely S/TPK/RK/R, AAKK/AKKA, PKAAKP, and K/RPK/R, are also shown. The histone octapeptide motif is shown in italics. (B) Secondary structures of histone H1 subtypes as predicted by CF and GOR algorithms. Note the motif helix(1)-turn-helix(3)-turn-helix(3) between residues 40 and 85 in histone H1d which is different in histone H1t. Also, note the long stretches of β-turns in the C-terminal tail of histone H1t.

which are active in DNA replication, while histone H1t is actively transcribed in pachytene spermatocytes (Meistrich et al., 1985). For a comparison, we have used histone H1bdec preparation from liver. According to the results of Lennox and Cohen (1983), the liver from 60-day-old rats has the histones H1a and H1b at very low levels while histone H1d is decreasing in amount. At this age, histones H1c and H1e are the major histone H1 subtypes present in this tissue. Among the various histone H1 subtypes of rat, the complete amino acid sequences of only histones H1d (Cole et al., 1990; Drabent et al., 1993) and H1t (Cole et al., 1986) have been determined. Baubichon-Cortay et al. (1992) have reported partial amino acid sequences of the globular domains of rat histones H1a and H1b (residues 34−153). It is interesting to note from the reported sequences that, while histones H1b and H1d showed 85% similarity to each other, histone H1a showed considerable divergence (60% similarity with histones H1b and H1d). It is, therefore, apparent that an exhaustive comparison of the sequences of all the histone H1 subtypes of rat is not possible at present. In their paper on histone H1d sequence, Cole et al. (1990) have indicated that their histone H1d corresponds to histone H1e of Lennox and Cohen (1983). Therefore, in our histone H1bdec preparation from rat liver, histone H1d should be one of the major constituents. The sequences of rat histone H1d and histone H1t are shown in Figure 9A. It is evident that most of the differences between these two subtypes are confined to the sequences of the C-terminal tails. The secondary structure predictions based on CF and GOR algorithms are given in Figure 9B. From a careful examination of these theoretical predictions, three observations can be made. (a) The potential helical content in the C-terminal half of histone H1t is less than that of histone H1d. (b) There are longer stretches of β-turn in histone H1t than in histone H1d. (c) Histone H1d contains a helix(1)-turn-helix(2)-turn-helix(3) in the globular domain between the amino acid residues 40 and 85. This predicted structure has recently been confirmed by NMR studies of histone GH1 (Cerf et al., 1993) and the crystal structure of chicken histone GH5 (Ramakrishnan et al., 1993). This motif is similar to the DNA binding homeodomain in *Drosophila antennapedia* protein (Mannerma et al., 1990), and hence, it has been suggested that this may be the DNA-recognizing motif that interacts with the chromatosome particle. Surprisingly, the

same region in histone H1t contains, instead, helix(1)-turn-helix (2). The significance of this difference, if any, cannot be addressed at present. The availability of the amino acid sequences of histones H1d and H1t, therefore, has allowed us to interpret the differences in the DNA-condensing properties of the testis specific histone H1t compared with that of somatic histone H1s.

In some of the original studies, acid-extracted histone H1s were used to investigate the DNA-condensing properties of histone H1 (Liao & Cole, 1981; Fasman et al., 1970; Mura & Stollar, 1972). However, Brand et al. (1981) and Garcia Ramirez et al. (1990) reported that salt-extracted histone H1s differ in their secondary structure from acid-extracted proteins as revealed by circular dichroism spectroscopy. Before making a detailed analysis of the DNA-condensing properties of histone H1 subtypes, we investigated the method of isolation of these histone H1 subtypes. A systematic study of the secondary structure characteristics of the histone H1 subtypes isolated using acid extraction and salt extraction procedures reported here reemphasizes the notion that the acid-extracted histone H1s may be partially denatured in an irreversible manner and hence may not have optimum and physiologically meaningful DNA binding properties. Our results have clearly shown that the secondary structural characteristics of both the globular domain and the C-terminal tail in the presence of 60% TFE of acid-extracted histone H1 subtypes are significantly affected. The impairment of the secondary structural characteristics of acid-extracted histone H1s was also reflected in their ability to condense duplex DNA in comparison with salt-extracted histone H1 subtypes (Figure 5). There was almost a 10-fold difference in the net condensation (as measured by $\Delta\theta$ at 270 nm) of rat oligonucleosomal DNA observed between the salt- and acid-extracted histone H1s.

We observed another striking difference between the acid- and salt-extracted histone H1s with respect to the number of base pairs of DNA occupied per histone H1 molecule. An occupancy size of 16−20 bp was calculated for the salt-extracted histone H1 which was increased to an apparent size of 160−200 bp for acid-extracted histone H1. Thomas and Widom and their co-workers have done elegant studies on the nature of interaction of salt-extracted histone H1 with DNA (Clark & Thomas, 1986, 1988; Draves et al., 1992). Histone H1 binds to DNA in a cooperative fashion, above 35 mM NaCl, through its globular domain to form thick bundles 11−15 nm in diameter that forms a tramlike structure wherein histone H1 molecules are packed between two DNA duplexes (Clark & Thomas, 1986, 1988). An occupancy size of 47 bp was calculated per histone H1 molecule in such structures. Draves et al. (1992) have shown that the globular domain of histone H5 binds to DNA in a cooperative manner with an occupancy of size of 8−9 bp/mole of the globular domain. They have further shown that GH5 molecules are in close proximity to each other by chemical cross-linking experiments. The occupancy size of 16−20 base pairs that we have calculated in the present study falls between the two values reported by these workers for the intact histone H1 molecule and the globular domain. The observation that the acid-extracted histone H1 showed an apparent occupancy size of 160−200 bp suggests that the globular domains are partially denatured in the acid-extracted proteins. We have also arrived at an apparent occupancy size ranging from 120 to 200 bp for the acid-extracted histone H1 molecules from the data reported in the literature (Mura et al., 1972; Fasman et al., 1970). These numbers, therefore, suggest that the partial denaturation of the globular domain in the acid-extracted histone H1 would probably hamper close packing of the histone H1 molecules between the two DNA duplexes. A significant decrease in the net condensation observed with acid-extracted histone H1s as compared to that with the salt-extracted histone H1s is probably a reflection of this impairment of loading of H1 molecules on the DNA. We would also like to point out that the structure of the C-terminal tail, which is the DNA-condensing domain in histone H1 (Moran et al., 1985), as measured indirectly in the presence of 60% TFE, is also affected by acid extraction (Table 1). The significance of this difference on the condensation property cannot be ascertained at present. Our results on the comparative analysis of the DNA-condensing properties of histones H1bdec, H1a, and H1t have clearly shown that histone H1bdec has the maximum condensing property, followed by histone H1a. The testis specific variant has the least DNA-condensing property. Such a difference in the condensation property was also reflected with histone H1-depleted chromatin. In fact, there was very little change in the CD spectrum of H1-depleted chromatin after addition of histone H1t. While these studies were in progress, Delucia et al. (1994) came to similar conclusions, however, with acid-extracted histone H1 subytpes.

Although we cannot comment on the significance of increased expression of histone H1a in replicating cells on the basis of the results we have obtained here, we can definitely make some predictions with respect to histone H1t. Due to its poor DNA- and chromatin-condensing properties, histone H1t-interacting chromatin domains in pachytene spermatocytes might have a more open conformation so as to facilitate specific meiotic prophase-associated events. We had come to a similar conclusion on the basis of the elution properties of different histone H1 subtypes from rat testes chromatin-bound to hydroxylapatite (Khadake et al., 1994).

The next obvious question that arises is what is the information that is present in histone H1bdec but absent in histone H1t that is responsible for generating highly ordered aggregates of DNA complexes? As mentioned earlier, Moran et al. (1985) have shown that it is the C-terminal domain of histone H1 which is responsible for generating the ψ type of spectrum. Since histone H1d is the predominant histone H1 subtype present in our preparation of H1bdec (as discussed above) and its amino acid sequence (Cole et al., 1990; Drabent et al., 1993) as well as that of histone H1t (Cole et al., 1986) are available, we have made a careful analysis of the different DNA binding motifs present in their C-terminal tail (Figure 9). An octapeptide motif of the type KSPKKAKK is repeated many times in the C-terminus of somatic histones (Tonjes & Doenecke, 1987). Erard et al. (1990) have shown that one such motif KSPKKAKKP can generate a strong ψ type spectrum when present as a tandem repeat at a peptide/DNA ratio of 0.66 mole/bp . From Figure 9, one can notice that histone H1d has three such closely related octapeptide motifs in the C-terminal region of the molecule, of which two form a direct repeat (A^{144}-TPKKSTKKTPKKAKK^{159} and K^{170}SPKKAKA^{177}). Interestingly, such an octapeptide motif is absent in histone H1t. We have also observed additional differences in the frequency of occurence of several DNA binding motifs, which were recently discussed by Churchill and Travers (1991),

Table 2: DNA Binding Motifs Present in Different Histone H1s[a]

DNA binding motif	H1 subtype	number of repeat units
S/TPKK	H1d	3
	H1t	0
AAKK/AKKA	H1d	5
	H1t	0
PKAAKP	H1d	2
	H1t	0
K/RPK/R	H1d	6
	H1t	2

[a] Various DNA binding motifs present in histone H1, discussed by Churchill and Travers (1991), were scanned in the amino acid sequences of histones H1t and H1d (shown in Figure 9A).

between histone H1d and H1t. They are summarized in Table 2. It is clear from the table that histone H1t lacks most of these motifs. There are no S/TPK/RK/R, AAKK/AKKA, or PKAAKP motifs at all in histone H1t as against three, five, and two repeats, respectively, in histone H1d. Histone H1t has two repeats of K/RPK/R. Of these two repeats, one is in the C-terminal tail while the other is in the N-terminal tail. The lack of several of the DNA binding motifs in histone H1t is very striking. It is therefore possible that the lack of these DNA binding motifs in histone H1t coupled with substantial β-turns in its C-terminal tail (Figure 9) might contribute to the lack of its chromatin-condensing properties. It would be interesting to study the finer localization of histone H1t in pachytene spermatocyte chromatin and to examine the DNA transaction processes that are influenced by such a "loosened" chromatin structure.

ACKNOWLEDGMENT

Jyoti R. Khadake was a Senior Research Fellow of Council of Scientific and Industrial Research. We thank Dr. Udgoankar of the National Centre for Biological Sciences, TIFR, and Dr. K. R. K. Easwaran of the Molecular Biophysics Unit, for providing the use of the JASCO 500A and JASCO J20 spectropolarimeters, respectively.

REFERENCES

Allan, J., Mitchell, T., Harborne, N., Bohm, L., & Crane-Robinson, C. (1986) *J. Mol. Biol. 187*, 591−601.
Allan, J., Staynov, D. Z., & Gould, H. (1990) *Proc. Natl. Acad. Sci. U.S.A. 84*, 885−889.
Baubicon-Cortay, H., Mallet, L., Deneroy, L., & Roux, B. (1992) *Biochim. Biophys. Acta 1122*, 167−177.
Brand, S. H., Kumar, N. M., & Walker, I. O. (1981) *FEBS Lett. 133*,63−68.
Camerini-Otero, R. D., Sollner-Webb, B., & Felsenfeld, G. (1976) *Cell 8*, 333−347.
Cerf, C., Lippens, G., Muyldermans, S., Segers, A., Ramamkrishnan, V., Wodak, S., Hallenga, K., & Wyns, L. (1993) *Biochemistry 32*, 11345−11351.
Churchill, M. E. A., & Travers, A. A. (1991) *Trends Biochem. Sci. 16*, 92−97.
Clark, D. J., & Thomas, J. O. (1986) *J. Mol. Biol. 187*, 569−580.
Clark, D. J., & Thomas, J. O. (1988) *Eur. J. Biochem. 178*, 225−233.
Clark, D. J., Hill, C. S., Martin, S. R., & Thomas, J. O. (1988) *EMBO J. 7*, 69−75.
Clore, G. M., Groneborn, A. M., Nilges, M., Sukumaran, D. K., & Zarbock, J. (1987) *EMBO J. 6*, 1833−1842.
Cole, K. D., Kandala, J. C., & Kistler, W. S. (1986) *J. Biol. Chem. 261*, 7718−7183.
Cole, K. D., Kandala, J. C., Kremer, E., & Kistler, W. S. (1990) *Gene 89*, 265−269.
Cole, R. D. (1987) *Int. J. Pept. Protein Res. 30*, 433−449.
Delucia, J., Faraone-Mannella, M. R., D'Erme, M., Quesada, P., Caiafa, P., & Farina, B. (1994) *Biochem. Biophys. Res. Commun. 198*, 32−39.
De Petrocellis, L., Quagliarotti, G., Tomei, L., & Geraci, G. (1986) *Eur. J. Biochem. 156*, 143−148.
Drabent, B., Kardilinole, E., & Doenecke, D. (1991) *Gene 103*, 263−268.
Drabent, B., Kunz, C., & Doenecke, D. (1993) *Biochim. Biophys. Acta 1172*, 193−196.
Draves, P. H., Lowary, P. T., & Widom, J. (1992) *J. Mol. Biol. 225*, 1105−1121.
Erard, M., Lakhdar-Ghazal, J., & Amalric, J. (1990) *Eur. J. Biochem. 191*, 19−25.
Fasman, G. D., Schaffhausen, B., Golsmith, L., & Adler, A. (1970) *Biochemistry 9*, 2814−2822.
Garcia-Ramirez, M., Leuba, S. H., & Ausio, J. (1990) *Protein Expression Purif. 1*, 40−44.
Johns, E. W., & Butler, J. A. V. (1962) *Biochem. J. 82*, 15−18.
Jordan, C. J., Lerman, L. S., & Venables, J. H., Jr. (1972) *Nature, New Biol. 236*, 67−70.
Kas, E., Izaurralde, E., & Laemmli, U. K. (1989) *J. Mol. Biol. 210*, 573−599.
Khadake, J. R., Markose, E. R., & Rao, M. R. S. (1994) *Indian J. Biochem. Biophys. 31*, 335−338.
Kremer, E., & Kistler, W. S. (1991) *Exp. Cell Res. 197*, 330−332.
Laemmli, U. K. (1970) *Nature 227*, 680−685.
Laybourn, P. J., & Kadanoga, J. T. (1991) *Science 254*, 238−245.
Lennox, R. W., & Cohen, L. H. (1983) *J. Biol. Chem. 258*, 262−268.
Liao, L. W., & Cole, R. D. (1981) *J. Biol. Chem. 256*, 6757−6755.
Mannerma, R. M., & Oikarinen, J. (1990) *Biochem. Biophys. Res. Commun. 168*, 254−260.
Markose, E. R., & Rao, M. R. S. (1985) *J. Biol. Chem. 260*, 16263−16268.
Meistrich, M. L., Bucci, R. L., Trostle-Weige, P. K., & Brock, W. A. (1985) *Dev. Biol. 112*, 230−240.
Moran, J., Montero, J., Azorin, J., & Suau, P. (1985) *Biophys. Chem. 22*, 125−129.
Mura, C. V., & Stollar, D. (1984) *Biochemistry 23*, 6147−6152.
Panyim, S., & Chalkely, R. (1969) *Arch. Biochem. Biophys. 130*, 337−341.
Platz, R. D., Meistrich, M. L., & Grimes, S. R., Jr. (1977) *Methods Cell Biol. 16*, 297−316.
Ramakrishnan, V., Finch, J. T., Graziano, V., Lee, P. L., & Sweet, R. M. (1993) *Nature 362*, 219−223.
Rao, M. R. S., Rao, B. J., & Ganguly, J. (1982) *Biochem. J. 205*, 15−21.
Renz, M. (1975) *Proc. Natl. Acad. Sci. U.S.A. 72*, 733−736.
Sambrook, J., Fritsch, E. F., & Maniatis, T. (1989) *Molecular Cloning*, Chapter 1.38−1.40, Cold Spring Harbor Press, Cold Spring Harbor, NY.
Thoma, J., Losa, R., & Koller, T. (1983) *J. Mol. Biol. 167*, 619−640.
Thomas, J. O., Rees, C., & Finch, J. T. (1992) *Nucleic Acid Res. 20*, 187−194.
Tonjes, R., & Doenecke, D. (1987) *J. Mol. Evol. 25*, 361−370.
Van Holde, K. E. (1988) *Chromatin*, Springer-Verlag, New York.
Varga-Weisz, P., Zaltanova, J., Leuba, S., Schroth, G. P., & Van Holde, K. E. (1994) *Proc. Natl. Acad. Sci. U.S.A. 91*, 3525−3529.
Weintraub, H. (1985) *Cell 42*, 705−711.
Weissbach, A., & Poonian, M. (1974) *Methods Enzymol. 34*, 463−475.
Wellman, S. E., Sittman, D. B., & Chaires, J. B. (1994) *Biochemistry 33*, 384−388.
Widom, J. (1989) *Annu. Rev. Biophys. Biophys. Chem. 18*, 365−395.

BI951258I